A novel variant in PAX6 as the cause of aniridia in a Chinese family

Xin Jin
Chinese PLA General Hospital
Wei Liu
Hainan Branch of Chinese PLA General Hospital
HouBin Huang (536273642@qq.com)
Chinese PLA General Hospital https://orcid.org/0000-0001-5076-1279
Linghui Qv
47st Hospital of Chinese People's Liberation Army
Wenqin Xv
301 Military Hospital: Chinese PLA General Hospital

Research article

Keywords: Aniridia, Autosomal dominant inheritance, PAX6 gene, Mutation

Posted Date: December 17th, 2020

DOI: https://doi.org/10.21203/rs.3.rs-21412/v3

Abstract

Background: Aniridia is a kind of congenital human pan-ocular anomaly, which is related to *PAX6* commonly.

Methods: The ophthalmic examinations including visual acuity, slit lamp and fundoscopy examination were performed in a Chinese aniridia pedigree. The targeted next-generation sequencing of aniridia genes was used to identify the causative mutation.

Results: A novel heterozygous *PAX6* nonsense mutation c.619A>T (p.K207*) was identified in the Chinese autosomal dominant family with aniridia. Phenotype related to the novel mutation included nystagmus, keratopathy, absence of iris, cataract and foveal hypoplasia.

Conclusion: The novel nonsense variation in *PAX6* was the cause of aniridia in this family, which expanded the spectrum of the *PAX6* mutation.

Background

Aniridia was a kind of rare congenital human ocular anomaly, it could manifest either as ocular abnormalities of iris hypoplasia, foveal hypoplasia, cataract, glaucoma, corneal dystrophy, as well as abnormalities of the optic nerve, or as syndromes of the WAGR syndrome (MIM#194072) and the Gillespie syndrome (MIM#206700)[1, 2]. The incidence of aniridia was between 1 per 50,000 and 96,000 births[3]. According to the difference of pathogenic genes, aniridia could be divided into three types, aniridia-1 (AN1, MIM #106210), aniridia-2 (AN2, MIM #617141) and aniridia-3 (AN3, MIM #617142). AN1 was caused by heterozygous mutation in the *PAX6* gene, AN2 was caused by heterozygous mutation in a *PAX6* cis-regulatory element that resides in an intron of the adjacent *ELP4* gene, and AN3 was caused by heterozygous mutation in the *TRIM44* gene[4, 5]. Some of the isolated aniridia was demonstrated due to mutations in *FOXC1* or *PITX2* genes. Mutations in these two genes were more commonly associated with juvenile onset glaucoma and anterior segment dysgenesis presenting with syndromic features of rare cardiac anomalies for *FOXC1* and hypodontia and umbilical anomalies for *PITX2*[6-8].

About one-third of the cases carry de novo variants[9]. The classic AN1 associated with *PAX6* haploinsufficiency presented iris hypoplasia and foveal hypoplasia, while heterozygous missense mutations in *PAX6* would lead to other ocular diseases including anterior segment dysgenesis and optic nerve malformations. *PAX6* (OMIM 607108), paired box gene 6, was a member of the paired box gene family which encodes a transcriptional regulator involved in oculogenesis and other developmental processes[10]. This transcription factor had shown functional conservation in developmental pathways. *PAX6* variant had been identified associated with aniridia and other ocular development abnormalities previously, while olfactory abnormalities and brain structure alterations in line with expression of Pax6 had also been documented recently[11]. *PAX6* played an important role in the process of development regulation which broadly expressed and was controlled by a number of long-range control elements and homozygous mutation led to more severe phenotype[11].

In the present study, we identified a novel heterozygous *PAX6* nonsense mutation c.619A>T (p.K207*) in a Chinese autosomal dominant family with aniridia. We used targeted next-generation sequencing (NGS) to screen all the genes related to iris diseases including aniridia and identified the causative mutations.

Methods

The Institutional Review Board (IRB) of Hainan hospital of Chinese PLA General Hospital (Hainan Province, China) approved the present study. All participating family members provided an informed written consent and were endorsed by their respective IRB. The whole procedure of the present study adhered to the tenets of the Declaration of Helsinki.

A small pedigree with aniridia from Hainan province, China, was recruited for the present study. This family included two affected and two unaffected members, which was analyzed and followed up clinically at Hainan Hospital of Chinese PLA General Hospital (Fig. 1A). Comprehensive ophthalmological examinations, including best correct visual acuity (BCVA), applanation tonometry, dilated funduscopy, anterior segment and fundus photography, ultrasound biomicroscopy (UBM) examination, gonioscopy and optical coherence tomography (OCT) of anterior segment and macular were performed on the affected individuals and the unaffected family members. Genomic DNA was collected from peripheral blood lymphocytes of the pedigree members and normal controls using a QIAamp DNA Blood Midi Kit (Qiagen, Hilden, Germany).

Targeted genes enrichment and sequencing

Target enrichment panel of specific hereditary eye based on the next generation sequencing was used to collect the protein-coding region of 371 targeted genes (designed by MyGenostics, Baltimore, MD), which included 37 genes associated with iris diseases. (*PAX6, ELP4, FOXD3, PITX3, FOXE3, PITX2, ADAMTS10, FBN1, LTBP2, ADAMTS17, MTHFR, TYR, MITF, PAX3, SNAI2, SOX10, RBP4, CHD7, TMEM67, RPGRIP1L, CC2D2A, YAP1, MAF, C12orf57, FOXC1, B3GLCT, NF1, GPR143, OCA2, TYRP1, CRYGC, ADAMTSL4, SALL2, IGBP1, CYP1B1, MYOC, SALL1*). The genes related to aniridia, WAGR syndrome, Axenfeld-Rieger syndrom and other diseases involved iris abnormity were covered. The process of specific high throughput sequencing was in conformity to some published articles[12, 13].

Bioinformatics analysis

After HiSeq 2000 sequencing, Solexa QA package and the Cutadapt program were used to filter out low quality reads and adaptor sequences and high-quality reads from raw reads were retrieved. Then the clean read sequences were aligned to the human reference genome (hg19) using SOA Paligner program. Subsequently, the single nucleotide polymorphism (SNPs) and the insertions or deletions (InDels) were identified using the SOAPsnp program and GATK program separately. The identified SNPs and InDels were annotated using ANNOVAR program (http://122. 228.158.106/exomeassistant) and viewed using MagicViewer. Finally, nonsynonymous variants were evaluated by four algorithms, Ployphen, SIFT, PANTHER and Pmut, as described previously to determine pathogenicity.

Mutation verification

After high throughput sequencing, the detected variations were validated by Sanger sequencing in the Chinese family. Primer6.0 was used to design the PCR primer sets and the PCR products were sequenced using a Bigdye terminator v3.1 cycle sequencing kit (ABI, Foster City, CA, USA) and analyzed on an ABI 3730XL Genetic Analyzer. The primers used in this study are listed in Table 1.

Results

Clinical Findings

There were two affected individuals, the proband and his mother, in this two-generation Chinese family (Fig. 1A). The inheritance pattern of the pedigree was in accordance with autosomal dominant inheritance. The proband (II:4) was a 29-year-old male, he felt blurred vision and photophobia in both eyes since childhood. His BCVA were 0.2 in right eyes and 0.15 in left eyes, with corrections of -4.25 diopters (D) in the right eye and -0.5 D in the left eye. Ophthalmic examination presented horizontal nystagmus, absence of almost whole iris, discrete posterior subcapsular cataract (Fig. 2A and 2B), and absence of macular central fovea (Fig. 3) in both eyes. The absence of iris was so severe that the equator of the lens and ciliary processes were exposed, which could be observed in anterior segment photography (Fig. 2B and 2F) and UBM examination (Fig. 2E). Anterior segment photograph demonstrated that the cornea of both eyes was transparent (Fig. 2A and 2B), but the central corneal thickness was 668μm in right eye and 664μm in left eye (Fig. 2C and 2D), which were slightly thicker than normal. The structure of anterior chamber angle could be observed under gonioscopy, and the anterior

chamber angle was open (Fig. 2F). The normal macula central fovea structure could not be found in fundus photograph and macular OCT (Fig. 3). Intraocular pressure of both eyes was normal. His mother had similar clinical symptoms and signs, moreover, her cataract became worse with age and she underwent phacoemulsification and intraocular lens implantation at 52 years old. There were no other systemic diseases except eye abnormalities in all the affects.

Identification of causing mutations

After filtering the candidate variants of the proband in the databases, a nonsense mutation *PAX6* c.619A>T in exon 8 changing codon 207 AAG to the stopcodon TAG (p.K207X) was detected. The mutation was absent in either databases mentioned earlier or reported literatures, which led to Lysine at 207 position in linker region transforming to a premature termination codon, and finally resulted in *PAX6* underdosage (Fig. 1B). Then the novel mutation was validated by Sanger sequencing and detected among the family members, which demonstrated that the *PAX6* c.619A>T heterozygous mutation was cosegregated with the aniridia phenotype in this family (Fig. 1A). The affected individuals, the proband and his mother, carried the mutation, while the unaffected members did not. These results suggested that *PAX6* c.619A>T was a novel causative mutation for autosomal dominant congenital aniridia.

Discussion

Aniridia associated with mutations in PAX6 was categorized into classic aniridia group, while that associated with mutations in genes other than *PAX6* was aniridia-like group[7, 8]. Classic aniridia referred to a pan-ocular disorder, including partial or near total absence of iris, cataract, aniridia-associated keratopathy (ARK), glaucoma, foveal hypoplasia, optic disk hypoplasia and nystagmus[14-16]. Iris hypoplasia was the most important feature of aniridia, which could range from complete absence of the iris, through enlargement and irregularity of the pupil mimicking a coloboma, to small slit-like defects in the anterior layer seen only on transillumination with a slit-lamp. The incidence of other features of classic aniridia was different, nystagmus was 76%, cataract was 56%, glaucoma was 64% and visible keratopathy was 80%[17]. In this study, we identified the pathogenic gene mutation in a Chinese aniridia family using an iris diseases panel including 37 targeted genes. The patients in this family presented nystagmus, ARK, absence of iris, cataracts and foveal hypoplasia. Then a novel *PAX6* nonsense mutation c.619A>T (p.K207*) was identified and it was co-separated from disease phenotype.

A high proportion of cases of aniridia was associated with mutations in *PAX6* frameshift mutations, splicing site mutations or nonsense mutations and these kinds of variations have been considered to produce premature truncation of the protein or nonsense transcripts, leading to haploinsufficiency. While few cases were caused by missense mutations[16]. Aniridia phenotype associated with *PAX6* haploinsufficiency almost present anterior segment and fundus abnormalities, while missense mutations in *PAX6* were mostly associated with dysplasia of skeleton and central nervous system[18]. The most common clinical manifestations associated with aniridia haploinsufficiency were iris anomalies, nystagmus and foveal hypoplasia, followed by cataracts, glaucoma and corneal opacity. In this Chinese family, the phenotype was similar between the two patients. they both felt photophobia from childhood and exhibited nystagmus, ARK, aniridia, cataract and foveal hypoplasia. The novel mutation *PAX6* c.619A>T (p.K207*) in this family induced premature termination codons (PTCs) into the *PAX6* open reading frame, and the mRNAs containing PTCs were degraded by the nonsense-mediated decay process, which resulted in a single-dose deficiency. The phenotype associated with the novel mutation was in line with classic aniridia related to *PAX6* haploinsufficiency[16].

It was reported that the severity of iris hypoplasia varied in different *PAX6* cases and lens abnormalities include various degrees and types of cataracts and lens ectopic[16]. The patients of this Chinese family presented near total absence of iris and lamellar posterior subcapsular lens opacification without obvious lens ectopia. Keratopathy was common in aniridia patients as the PAX6 gene is responsible for embryonic and postnatal development of the cornea. At the early stage of keratopathy, the central corneal thickness increased, the basal epithelium became turbid and the corneal sensitivity

decreased. With the progression of the lesion, the cornea gradually became opacity from periphery area to apex[16]. In this family, the cornea of the proband remained transparent, but the central corneal thickness increased and the limbal vascular pannus indicated the presence of early ARK. Glaucoma in aniridia usually occurred in early adulthood, including infants and toddlers. It was caused by the irregular strands arising from the iris stroma attached to the angle wall. It was reported that a 24-year-old aniridia patient with *PAX6* c.607C>T, p.Arg203* presented glaucoma, the location of the mutation was very close to that of *PAX6* c.619A>T (p.K207*) , and these two gene locations were in the same domain[19]. However, the patients in this Chinese aniridia family were adults with normal intraocular pressure and no characteristic optic disc manifestations of glaucoma. They need follow-up observation of intraocular pressure to finally determine whether glaucoma will occur.

The human *PAX6* gene was cloned in 1991 and had been isolated from both vertebrates and invertebrates. It consisted of 14 exons and encodes a transcriptional regulator which had a paired-type DNA-binding domain. There were 2 distinct DNA-binding subdomains, the N-terminal subdomain (NTS) and the C-terminal subdomain (CTS), in the paired domain, which bind respective consensus DNA sequences to recognize target genes. The human *PAX6* gene produced 2 alternatively spliced isoforms that have the distinct structure of the paired domain[20]. There have been about 500 mutations reported in the human *PAX6* database[14] (https://www.ncbi.nlm.nih.gov/clinvar?term=607108[MIM]), since firstly identified as the genetic cause of aniridia in the small eye mouse[21]. While it was remarkable that the alterations in a conserved non-coding element within the “critical region” and other cis-regulatory elements also could cause aniridia[22]. *PAX6* whole-gene deletions and telomeric cis-regulatory elements deletions were also identified in some aniridia patients of negative for intragenic *PAX6* mutations. Consequently, it was suggested that *PAX6* whole-gene direct sequencing combined with and molecular methods of detecting copy number alterations (CNV) such as high-resolution comparative hybridization (HR-CGH) arrays, fluorescence in situ hybridization (FISH), and multiplex ligation-dependent probe amplification (MLPA) was important to improve detection rate for aniridia associated with *PAX6* variations, which could be more suitable for using in the aniridia cases of iris diseases panel screening negative[23]. It was thought greater locus heterogeneity might exist in both isolated and syndromic aniridia than was previously appreciated, therefore the improvement of detection method was helpful to improve the detection rate of pathogenic genes for aniridia. In this study, we just have screened protein-coding region of 37 genes associated iris diseases but ignored conserved non-coding element and CNV of *PAX6*, which should be improved in the future.

Conclusion

In brief, a novel nonsense mutation in *PAX6* (c.619A>T p.K207*) was identified in a Chinese family with aniridia, which could cause *PAX6* haploinsufficiency. The phenotype associated with this mutation included aniridia, ARK, cataracts and foveal hypoplasia. The present study expanded the mutation spectrum of the *PAX6* gene which may be helpful in the genetic diagnosis of aniridia.

Abbreviations

WAGR: Wilms tumor, aniridia, genitourinary anomalies and mental retardation syndrome; NGS: Next-generation sequencing; IRB: Institutional review board; BCVA: Best correct visual acuity; UBM: Ultrasound biomicroscopy; OCT: optical coherence tomography; PAX6: Paired box gene 6; ELP4:Elongator acetyltransferase complex subunit 4; FOXD3: Forkhead box D3; PITX3: Paired-like homeodomain transcription factor 3; FOXE3:Forkhead box E3; PITX2: Paired-like homeodomain transcription factor 2; ADAMTS10: A disintegrin-like and metalloproteinase with thrombospondin type 1 motif, 10; FBN1: Fibrillin 1; LTBP2:Latent transforming growth factor-beta-binding protein 2; ADAMTS17: A disintegrin-like and metalloproteinase with thrombospondin type 1 motif, 17; MTHFR: Methylenetetrahydrofolate reductase; TYR:Tyrosinase; MITF:Microphthalmia-associated transcription factor; PAX3: Paired box gene 3; SNAI2: Snail family transcriptional repressor 2; SOX10: Sry-box 10; RBP4:Retinol-binding protein 4; CHD7:Chromodomain helicase dna-binding protein 7; TMEM67: Transmembrane protein 67; RPGRIP1L: Rpgrip1-like; CC2D2A: Coiled-coil and c2 domains-containing protein 2a;

YAP1: Yes-associated protein 1, 65-kd; MAF: Maf bzip transcription factor; C12orf57: Chromosome 12 open reading frame 57; FOXC1: Forkhead box c1; B3GLCT: Beta-3-glucosyltransferase; NF1: Neurofibromin 1; GPR143: G protein-coupled receptor 143; OCA2: Oca2 melanosomal transmembrane protein; TYRP1: Tyrosinase-related protein 1; CRYGC: Crystallin, gamma-c; ADAMTSL4: Adamts-like 4; SALL2: Sal-like 2; IGBP1: Immunoglobulin-binding protein 1; CYP1B1: Cytochrome p450, subfamily i, polypeptide 1; MYOC: Myocilin; SALL1: Sal-like 1; SNPs: Single nucleotide polymorphism; PCR: Polymerase chain reaction; PTC: Premature termination codon; NTS: N-terminal subdomain; CTS: C-terminal subdomain; CNV: Copy number alterations; HR-CGH: High-resolution comparative hybridization; FISH: Fluorescence in situ hybridization; MLPA: Multiplex ligation-dependent probe amplification;

Declarations

Ethics approval and consent to participate This study followed the tenets of the Declaration of Helsinki and conducted with approval from the Ethics Committee of the Hainan hospital of Chinese PLA General Hospital. A written informed consent was obtained from each participant.

Consent to publish All the patients had written informed consent for the publication of this article and all accompanying images.

Availability of data and materials All data generated and analyzed during this study were included in this manuscript.

Competing interests The authors declared that they have no conflict of interest.

Funding: The funds needed for the sequencing experiment were supported by Hainan Natural Science Foundation (NO. 817347).

Authors' Contributions Conceived and designed the work: HB Huang and X Jin. Data analyzed the work: X Jin, W Liu and LH Qv. Drafted the work: X Jin and W Liu. Substantively revised the work: X Jin and WQ Xu.

Acknowledgements The authors would like to thank all the patients and their family.

The authors were also grateful to Dr. MR Xue and Dr. Y Wang, for they performing the ophthalmic examinations.

References

1. Breslow NE, Takashima JR, Ritchey ML, Strong LC, Green DM: **Renal failure in the Denys-Drash and Wilms' tumor-aniridia syndromes**. *Cancer Res* 2000, **60**(15):4030-4032.
2. Gerber S, Alzayady KJ, Burglen L, Bremond-Gignac D, Marchesin V, Roche O, Rio M, Funalot B, Calmon R, Durr A *et al*: **Recessive and Dominant De Novo ITPR1 Mutations Cause Gillespie Syndrome**. *Am J Hum Genet* 2016, **98**(5):971-980. doi:10.1016/j.ajhg.2016.03.004
3. Boonstra N, Limburg H, Tijmes N, van Genderen M, Schuil J, van Nispen R: **Changes in causes of low vision between 1988 and 2009 in a Dutch population of children**. *Acta Ophthalmol* 2012, **90**(3):277-286. doi:10.1111/j.1755-3768.2011.02205.x
4. Lauderdale JD, Wilensky JS, Oliver ER, Walton DS, Glaser T: **3' deletions cause aniridia by preventing PAX6 gene expression**. *Proc Natl Acad Sci U S A* 2000, **97**(25):13755-13759. doi:10.1073/pnas.240398797
5. Zhang X, Qin G, Chen G, Li T, Gao L, Huang L, Zhang Y, Ouyang K, Wang Y, Pang Y *et al*: **Variants in TRIM44 Cause Aniridia by Impairing PAX6 Expression**. *Hum Mutat* 2015, **36**(12):1164-1167. doi:10.1002/humu.22907
6. Ito YA, Footz TK, Berry FB, Mirzayans F, Yu M, Khan AO, Walter MA: **Severe molecular defects of a novel FOXC1 W152G mutation result in aniridia**. *Invest Ophthalmol Vis Sci* 2009, **50**(8):3573-3579. doi:10.1167/iovs.08-3032
7. Sadagopan KA, Liu GT, Capasso JE, Wuthisiri W, Keep RB, Levin AV: **Anirdia-like phenotype caused by 6p25 dosage aberrations**. *Am J Med Genet A* 2015, **167A**(3):524-528. doi:10.1002/ajmg.a.36890

8. Khan AO, Aldahmesh MA, Alkuraya FS: **Genetic and genomic analysis of classic aniridia in Saudi Arabia**. *Mol Vis* 2011, **17**:708-714.
9. Vincent MC, Pujo AL, Olivier D, Calvas P: **Screening for PAX6 gene mutations is consistent with haploinsufficiency as the main mechanism leading to various ocular defects**. *Eur J Hum Genet* 2003, **11**(2):163-169. doi:10.1038/sj.ejhg.5200940
10. Pedersen HR, Baraas RC, Landsend ECS, Utheim OA, Utheim TP, Gilson SJ, Neitz M: **PAX6 Genotypic and Retinal Phenotypic Characterization in Congenital Aniridia**. *Invest Ophthalmol Vis Sci* 2020, **61**(5):14. doi:10.1167/iovs.61.5.14
11. Hever AM, Williamson KA, van Heyningen V: **Developmental malformations of the eye: the role of PAX6, SOX2 and OTX2**. *Clin Genet* 2006, **69**(6):459-470. doi:10.1111/j.1399-0004.2006.00619.x
12. Ying J, Lin C, Wu J, Guo L, Qiu T, Ling Y, Shan L, Zhou H, Zhao D, Wang J *et al*: **Anaplastic Lymphoma Kinase Rearrangement in Digestive Tract Cancer: Implication for Targeted Therapy in Chinese Population**. *PLoS One* 2015, **10**(12):e0144731. doi:10.1371/journal.pone.0144731
13. Jin X, Chen L, Wang D, Zhang Y, Chen Z, Huang H: **Novel compound heterozygous mutation in the POC1B gene underlie peripheral cone dystrophy in a Chinese family**. *Ophthalmic Genet* 2018, **39**(3):300-306. doi:10.1080/13816810.2018.1430239
14. Lima Cunha D, Arno G, Corton M, Moosajee M: **The Spectrum of PAX6 Mutations and Genotype-Phenotype Correlations in the Eye**. *Genes (Basel)* 2019, **10**(12). doi:10.3390/genes10121050
15. Wang P, Sun W, Li S, Xiao X, Guo X, Zhang Q: **PAX6 mutations identified in 4 of 35 families with microcornea**. *Invest Ophthalmol Vis Sci* 2012, **53**(10):6338-6342. doi:10.1167/iovs.12-10472
16. Lagali N, Wowra B, Fries FN, Latta L, Moslemani K, Utheim TP, Wylegala E, Seitz B, Kasmann-Kellner B: **PAX6 Mutational Status Determines Aniridia-Associated Keratopathy Phenotype**. *Ophthalmology* 2020, **127**(2):273-275. doi:10.1016/j.ophtha.2019.09.034
17. Samant M, Chauhan BK, Lathrop KL, Nischal KK: **Congenital aniridia: etiology, manifestations and management**. *Expert Rev Ophthalmol* 2016, **11**(2):135-144. doi:10.1586/17469899.2016.1152182
18. Azuma N, Yamaguchi Y, Handa H, Tadokoro K, Asaka A, Kawase E, Yamada M: **Mutations of the PAX6 gene detected in patients with a variety of optic-nerve malformations**. *Am J Hum Genet* 2003, **72**(6):1565-1570. doi:10.1086/375555
19. Dubey SK, Mahalaxmi N, Vijayalakshmi P, Sundaresan P: **Mutational analysis and genotype-phenotype correlations in southern Indian patients with sporadic and familial aniridia**. *Mol Vis* 2015, **21**:88-97.
20. Glaser T, Walton DS, Maas RL: **Genomic structure, evolutionary conservation and aniridia mutations in the human PAX6 gene**. *Nat Genet* 1992, **2**(3):232-239. doi:10.1038/ng1192-232
21. Hill RE, Favor J, Hogan BL, Ton CC, Saunders GF, Hanson IM, Prosser J, Jordan T, Hastie ND, van Heyningen V: **Mouse Small eye results from mutations in a paired-like homeobox-containing gene**. *Nature* 1992, **355**(6362):750. doi:10.1038/355750a0
22. Bhatia S, Bengani H, Fish M, Brown A, Divizia MT, de Marco R, Damante G, Grainger R, van Heyningen V, Kleinjan DA: **Disruption of autoregulatory feedback by a mutation in a remote, ultraconserved PAX6 enhancer causes aniridia**. *Am J Hum Genet* 2013, **93**(6):1126-1134. doi:10.1016/j.ajhg.2013.10.028
23. Ansari M, Rainger J, Hanson IM, Williamson KA, Sharkey F, Harewood L, Sandilands A, Clayton-Smith J, Dollfus H, Bitoun P *et al*: **Genetic Analysis of 'PAX6-Negative' Individuals with Aniridia or Gillespie Syndrome**. *PLoS One* 2016, **11**(4):e0153757. doi:10.1371/journal.pone.0153757

Tables

Table 1. Primers used for potential pathogenic mutations amplification

Mutation	Gene	Exon	Forward primer (5′-3′)	Reverse primer (5′-3′)
c.619A>T	*PAX6*	8	TCAGACATTTAGTCTTTGAATTACTGG	GAGTTTAAGACTACACCAGGCCC

Figures

Fig1

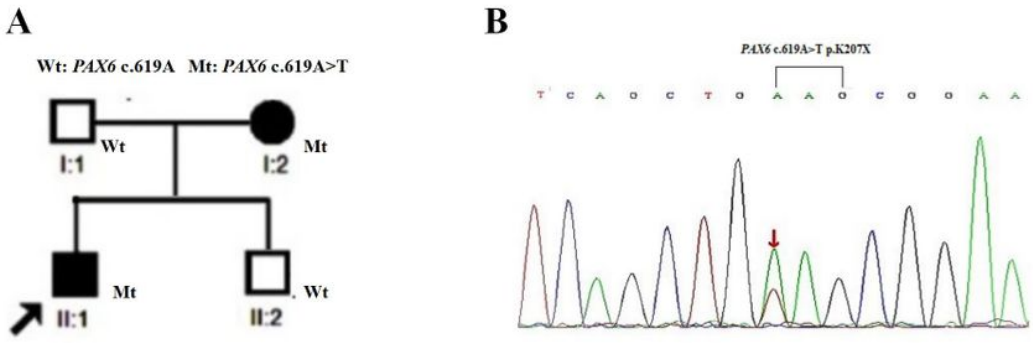

Fig 1. Identification of the heterozygous mutation c.619A>T in *PAX6* in a Chinese family with aniridia. (**A**) Pedigree of the family. Squares indicated males and circles indicated females. Empty symbols and filled symbols represented the normal and affected individuals , respectively.Wt: wild-type and Mt: mutation. The black arrow indicated the proband. (**B**) Sequence chromatograms showing the PAX6 c.619A>T mutation identified in this study. The red arrow indicated the site of the mutation.

Figure 1

Caption found in figure.

Fig2

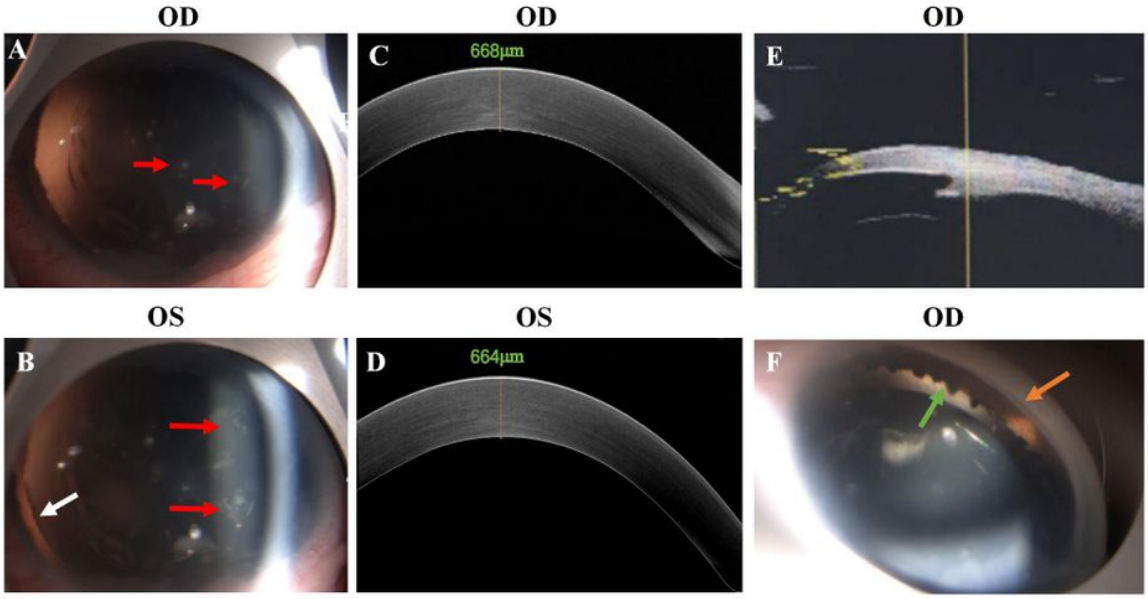

Fig 2. Anterior segment features of the proband in the family with aniridia. **(A and B)** Slit-lamp photographs of proband. The white arrow indicated the equator of lens and the red arrows indicated discrete posterior subcapsular cataract. **(C and D)** Cornea OCT examination of proband. **(E)** Ultrasound biomicroscopy examination of proband's right eye. **(F)** Anterior gonioscopy photographs. The green arrow indicated ciliary process and the orange arrow showed the structure of anterior chamber angle. OD stands for right eye, OS, left eye.

Figure 2

Caption found in figure.

Fig3

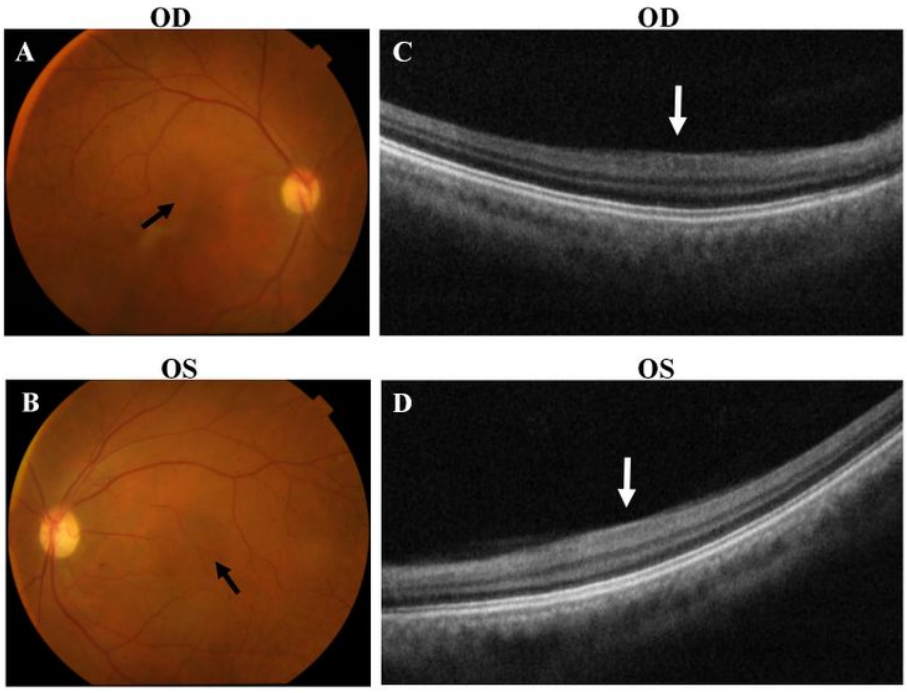

Fig 3. Fundus examination of the proband in the family with aniridia. **(A and B)** Fundus photography of proband. The black arrows showed the structure of macular area. **(C and D)** Macular OCT examination of proband.The white arrows indicated the structure of fovea of macula. OD stands for right eye, OS, left eye.

Figure 3

Caption found in figure.

Fig4

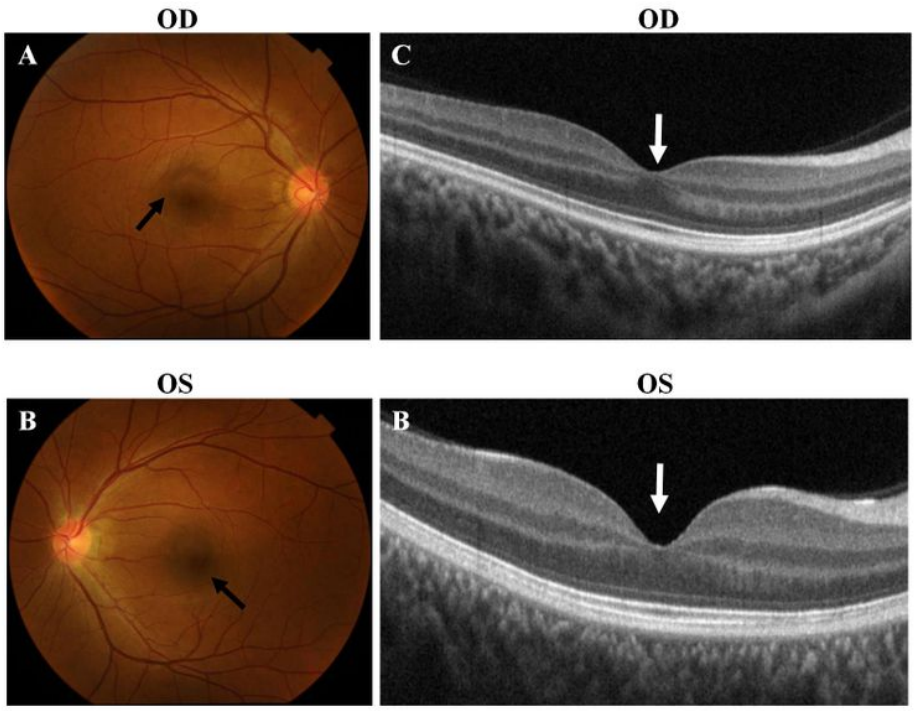

Fig 4. Fundus examination of the normal control. **(A and B)** Fundus photography of the normal control. The black arrows showed the structure of macular area. **(C and D)** Macular OCT examination of the normal control.The white arrows indicated the structure of fovea of macula. OD stands for right ey, OS, left eye.

Figure 4

Caption found in figure.